Math. Appl. 14(2)2025, 104–130

A Hybrid Quantum Differential Evolution Algorithm for Cost-Optimal Scheduling of Appliances and Energy Storage in PV-Equipped Smart Homes

Gursleen Kaur[1*] , Rajesh Kumar Bawa[2]

Abstract: *Minimising the daily electricity cost of a household equipped with rooftop photovoltaic (PV) panels and a stationary energy storage system (ESS) requires appliance scheduling and storage dispatch to be optimised jointly under a day-ahead tariff. The resulting problem is of a mixed discrete–continuous nature: it combines integer appliance start times with continuous charge and discharge commands, and it is coupled across successive hours through the stored energy. This paper proposes a hybrid quantum differential evolution (HQDE) algorithm for this cost-minimisation problem. HQDE directs its differential mutation towards an elite subset of the population using control parameters that are scheduled over the run, and it additionally explores the appliance variables in a quantum-inspired angle space while retaining the storage commands in their physical units. Each candidate solution is decoded into an appliance schedule that always satisfies the required operating hours, and a fixed allocation order coordinates PV generation, ESS operation and grid exchange in every hour. Over 50 independent runs on a common simulator, HQDE reduced the mean daily cost of improved differential evolution (IDE), the strongest of four baseline algorithms, by 9.75% for a benchmark household, and even its worst run outperformed the best run of every baseline. HQDE also achieved a lower mean cost than IDE in all six storage configurations examined, and these configurations further revealed that the charge/discharge rate of the ESS influences the minimum cost more strongly than its capacity. A sensitivity analysis over 18 combinations of PV size, selling-price coefficient and storage rate showed that PV size has the greatest impact on cost and that the selling coefficient becomes most influential when PV generation is abundant.*

Introduction

Residential electricity demand is increasingly subject to tariffs that vary from hour to hour. When the price of grid energy depends on the time of use, a household can reduce its bill by shifting flexible consumption away from high-price hours, and the smart grid provides the bidirectional communication infrastructure that conveys such price signals to consumers [1]. Demand-side management (DSM) programmes exploit these signals to influence both the timing and the magnitude of electricity consumption [2], [3]. At the household level, DSM is implemented through a home energy management system (HEMS), which receives the tariff and device data and determines when each controllable device operates [4], [5].

[1,2]Department of Computer Science, Punjabi University, Patiala, Punjab 147002, India

[*]Corresponding author: Gursleen Kaur (E-mail: gursleen109@gmail.com).

Keywords: *Appliance scheduling, cost minimisation, differential evolution, energy storage system, home energy management system, photovoltaic generation, quantum-inspired optimisation.*

From the household's perspective, the daily electricity cost is the most direct measure of the value delivered by a HEMS, and cost-minimising scheduling constitutes the fundamental problem from which richer formulations are derived [8], [9]. The cost-optimal schedule, however, is highly sensitive to the installed equipment and to the tariff.

The scheduling task has grown in complexity as households adopt distributed energy resources. Rooftop photovoltaic (PV) panels supply part of the daytime demand, and a stationary energy storage system (ESS) shifts energy from low-price or high-irradiance hours to high-price hours [6], [7]. These resources broaden the potential for cost savings, but they also alter the structure of the optimisation problem: appliance start times are integer-valued, storage commands are continuous, and the energy stored in one hour constrains all subsequent hours. A schedule that neglects any of these features may appear economical in theory but cannot be implemented in practice.

The capacity and charge/discharge rate of the ESS limit the amount of energy that can be shifted, the size of the PV array determines the surplus available for storage, and the ratio of the selling price to the purchase price determines whether exporting stored energy is profitable. A rigorous study should therefore quantify these effects in addition to evaluating the performance of the optimiser.

Population-based metaheuristics are the prevailing tools for this class of problem because they require neither gradient information nor convex models. Genetic algorithms (GAs) and particle swarm optimisation (PSO) have been employed for appliance scheduling and for PV–ESS coordination [9]–[11], and differential evolution (DE) [12] and its improved variants have been applied to smart homes with PV and battery storage [13]. DE is well suited to the storage commands, since its mutation operator adds scaled differences of continuous vectors; however, its performance depends strongly on the mutation strategy and the control parameters [14], [15]. The appliance variables introduce an additional difficulty. When start positions are obtained by rounding and operating hours by ranking, large regions of the continuous search space decode to the same schedule, and a purely real-valued mutation may stagnate on these plateaus. Quantum-inspired evolutionary algorithms, which represent candidate values through angles and amplitudes, were introduced to preserve population diversity in such landscapes [16], [17]. Nevertheless, the selective application of such guidance to the appliance variables alone, within a DE framework for coordinated appliance and ESS scheduling, has not been investigated in the HEMS studies reviewed in Section II.

To address these issues, this paper proposes a hybrid quantum differential evolution (HQDE) algorithm for the cost-optimal day-ahead scheduling of such a household. The main contributions of this work are as follows.

- A cost-minimisation model is formulated for a smart home with five shiftable appliances, rooftop PV and a stationary ESS. A single signed command per hour governs both the charging and the discharging of the ESS, and a fixed allocation order assigns PV energy to the load, the ESS and wastage and directs stored energy either to the load or to the grid for sale, so that every candidate yields a unique, well-defined schedule.

- A continuous encoding is introduced in which each non-interruptible appliance is represented by a start variable and each interruptible appliance by a vector of priority scores. The associated deterministic decoder guarantees that the operating-hour and contiguity requirements are satisfied for every candidate, and it replaces 120 binary decisions with 51 continuous ones.
- The HQDE algorithm is proposed. It guides its differential mutation towards an elite subset using parameters scheduled over the run, applies a qubit-amplitude-inspired angle-space update exclusively to the appliance variables, and incorporates a late-stage best-guided phase and a stagnation-recovery mechanism.
- The proposed algorithm is benchmarked against four established methods, namely a GA, a hybrid of PSO and binary PSO (PSO+BPSO), standard DE and improved DE (IDE), on a common simulator with an identical evaluation budget and 50 independent runs per method. In addition, the study quantifies how the ESS capacity and rate, the PV size and the selling-price coefficient shape the minimum daily cost.

The remainder of this paper is organised as follows. Section II reviews the related literature. Section III formulates the household model and the cost-minimisation problem, and Section IV presents the proposed HQDE algorithm. Section V describes the experimental setup, Section VI presents and discusses the results, and Section VII concludes the paper and outlines directions for future research.

Related Work

Four strands of research are pertinent to this study: cost-oriented DSM formulations, metaheuristic appliance scheduling, the coordination of PV and storage in residential settings, and DE together with its adaptive and quantum-inspired extensions.

A. Cost-Oriented Demand-Side Management

Survey studies position the HEMS at the residential end of DSM and demand response (DR) and classify the tariffs, devices and control methods employed [2], [4], [5], [18]. Mohsenian-Rad et al. [3] formulated the consumption scheduling of multiple users as a game in which each user minimises its own payment, whereas Ma et al. [8] defined cost efficiency as the ratio of consumption benefit to payment and maximised it through fractional programming. Rasheed et al. [19] exploited real-time information and dynamic pricing to reduce cost and peak demand while respecting user preferences, Flores et al. [20] investigated demand planning in smart homes, Jamil et al. [21] coordinated appliances through game theory, and Iqbal et al. [22] managed the resources of a domestic microgrid. Stochastic and robust formulations have been developed to handle uncertainty in PV output and prices [23]. Although mathematical programming represents the constraints exactly, the model size grows rapidly when storage and nonlinear operating rules are introduced, which partly explains the widespread adoption of heuristic search for HEMS scheduling.

B. Metaheuristic Approaches to Appliance Scheduling

GAs are the most widely used heuristics in this domain. Irshad et al. [24] reported lower bills and a lower peak-to-average ratio (PAR) than those obtained under unscheduled operation, and Al-Duais et al. [10] applied a GA to real-time pricing with solar generation. PSO [25] was adopted by Chang and Wu [11] under time-of-use (ToU) pricing, while Rahim et al. [26] and Fatima et al. [27] compared a GA, binary PSO (BPSO), ant colony optimisation and other heuristics within energy management controllers. Cuckoo search [28], a hybrid of the dragonfly algorithm and a GA [29], an enhanced coati optimisation algorithm [30], an improved bald eagle search [31], a honey badger–dwarf mongoose hybrid [32] and several other heuristics [33], [34] have also been proposed. These studies typically report savings relative to unscheduled operation or to a small number of baselines; however, the comparisons rarely share a common model and evaluation budget, and many of them schedule appliances without considering storage.

C. Coordinated Scheduling of PV and Energy Storage

Dinh et al. [9] scheduled appliances, PV and an ESS using PSO and BPSO while permitting electricity sales to the grid. Ahmad et al. [35] integrated renewable generation and storage within an optimised HEMS, and Ali et al. [36] reduced grid consumption and cost under real-time pricing using a hybrid architecture. The sizing and operation of grid-connected PV–battery systems have been reviewed in [7]. Essiet et al. [13] applied an improved DE (IDE) to demand response in a smart home with rooftop PV and a battery bank, maximising user comfort and minimising PAR; this IDE serves as a baseline in the present study. In most of these works, the distinct roles of storage capacity and charge/discharge rate are not separated, and the algorithms are compared on different models and datasets.

D. Differential Evolution and Quantum-Inspired Optimisation

DE [12] generates mutant vectors from scaled differences of population members, recombines them with the parent vectors and retains the better vector of each parent–trial pair. Its sensitivity to the mutation strategy, scale factor and crossover rate has motivated an extensive body of research on parameter control [14], [15]. jDE allows each individual to carry and self-adapt its own parameters [37], JADE introduced current-to-p-best mutation with adaptive parameters and an optional external archive [38], and SHADE adapts the parameters on the basis of a historical memory of successful values [39]; Deng et al. [40] proposed a further self-adaptive variant. In energy applications, an enhanced DE has been applied to smart-grid energy management [41], an IDE with a secondary population archive to a smart home with PV and battery storage [13], and an updated DE with time-varying parameters to economic dispatch [42]. Quantum-inspired evolutionary algorithms encode candidates using qubit-like angles and update them through rotation [16], [17]. In residential scheduling, however, such guidance has not been integrated with DE in a manner that treats the quasi-discrete appliance variables differently from the physical storage commands.

E. Research Gaps and Positioning of This Study

Table 1 summarises the studies most closely related to this paper, from which three research gaps can be identified. First, the individual effects of ESS capacity, ESS rate, PV size and selling price on the cost-optimal schedule are rarely quantified within a single study. Second, algorithms are generally compared on different models and datasets, so that the reported differences conflate modelling effects with search effects. Third, the DE variants applied to HEMS treat the quasi-discrete appliance variables and the continuous storage commands with identical real-valued operators. This paper addresses these gaps by evaluating five algorithms with a common simulator, encoding and evaluation budget, by conducting a structured sensitivity analysis of the household equipment and tariff, and by restricting quantum-inspired guidance to the appliance variables.

TABLE 1. Studies closest to the present work

Study	Year	Method	Cost-related objective	Devices	Remark
[3]	2010	Game-theoretic scheduling	Payment of each user	Appliances of several users	Distributed scheduling among users
[8]	2016	Fractional programming	Cost efficiency	Appliances	Exact model that grows with the number of devices
[19]	2016	GA with dynamic pricing	Cost, PAR, comfort	Appliances	Price-responsive scheduling with user preferences
[13]	2019	IDE	Energy use, PAR, comfort	PV, battery and appliances	IDE baseline used here
[11]	2020	PSO	ToU cost	Appliances	Load shifting under ToU pricing
[9]	2020	PSO+BPSO	Cost, PAR	PV, ESS, grid selling	Selling of stored energy allowed
[24]	2020	GA	Cost, PAR	Appliances	Savings against unscheduled operation
[10]	2021	GA	Bill, PAR	PV and appliances	Real-time pricing
[32]	2023	Honey badger and dwarf mongoose	Cost, PAR	PV and ESS	Hybrid metaheuristic scheduling
[36]	2024	Hybrid optimisation	Grid use, cost	PV under real-time pricing	Reduced grid consumption and cost

System Model and Problem Formulation

The household is scheduled one day ahead over $T = 24$ hourly slots indexed by t, with $\Delta t = 1$ h, so that power and energy per slot are numerically equivalent and all energies are expressed in kWh. The notation is summarised in Table 2.

TABLE 2. Nomenclature

Symbol	Description
$\rho_{\text{buy}}(t), \rho_{\text{sell}}(t)$	Purchase and selling prices (\$/kWh)
α	Selling-price coefficient
$E_{\text{PV}}(t), k_{\text{PV}}$	PV energy and PV scaling factor
$E_{\text{fix}}(t), E_{\text{L}}(t)$	Fixed base load and total household load
$E_{\text{L}}^{\text{res}}(t)$	Load remaining after PV supply
P_a, h_a, τ_a	Rated power, required hours and start slot of appliance a
$x_a(t)$	ON/OFF status of appliance a in slot t
$\mathcal{A}_{\text{N}}, \mathcal{A}_{\text{I}}$	Non-interruptible and interruptible appliances
$u_{\text{E}}(t)$	Signed hourly command of the ESS
$c_{\text{E}}(t), d_{\text{E}}(t)$	Charging and discharging requests
$\hat{c}_{\text{E}}(t), D_{\text{E}}(t)$	Feasible charge and deliverable discharge
$R_{\text{E}}, \eta_{\text{E}}$	ESS rate limit (kWh/slot) and efficiency
$E_{\text{E}}(t)$	ESS energy at the end of slot t
$E_{\text{E}}^{\min}, E_{\text{E}}^{\max}$	Minimum and maximum stored energy
$E_{\text{E}}^{\text{init}}, E_{\text{E}}^{\text{term}}$	Initial and terminal stored energy
$E_{\text{grid}}(t), E_{\text{E}}^{\text{sell}}(t)$	Grid import and energy sold by the ESS
$E_{\text{PV}}^{\text{waste}}(t)$	PV energy that is neither used nor stored
$C_{\text{day}}, \widetilde{C}$	Daily cost and penalised daily cost
$W_{\text{PV}}, U_{\text{PV}}$	Daily PV wastage and PV utilisation
$V(\mathbf{z})$	Constraint-violation measure
$\mathbf{z}$	Decision vector
$NP, G_{\max}$	Population size and generation budget
F_i, CR_i	Scale factor and crossover rate of candidate i
$\theta_k, q(g)$	Angle of variable k and quantum blend weight

A. Household Configuration and Energy Flows

Fig. 1 illustrates the household configuration. The HEMS controller receives the day-ahead purchase tariff, the expected PV output and the household data, and it determines the operating times of the shiftable appliances and the hourly ESS commands. Fig. 2 depicts the energy paths permitted by the model. PV energy supplies the household load first, and any surplus may be used to charge the ESS. Because PV energy cannot be exported directly, any surplus that is neither consumed nor stored is wasted. The grid supplies the remaining load and may also charge the ESS. Energy discharged from the ESS serves the residual load, and any feasible discharge in excess of that load is sold to the grid. Apart from the explicit accounting of wasted PV energy, these rules follow the PV–ESS model with energy selling of [9].

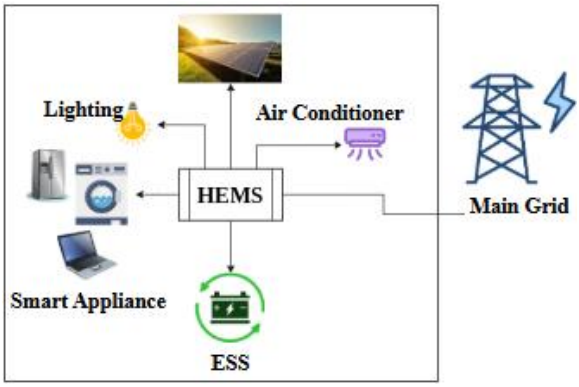


FIGURE 1. Smart household with shiftable appliances, PV generation, ESS and connection to the main grid.

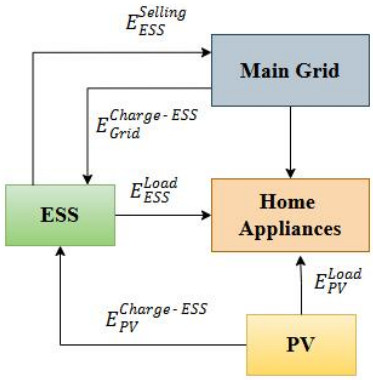


FIGURE 2. Energy paths among the main grid, PV system, ESS and household appliances.

B. Tariff and Photovoltaic Generation Models

Electricity is purchased at the day-ahead price $\rho_{\text{buy}}(t)$ and sold at a fixed fraction of this price:

$$\rho_{\text{sell}}(t) = \alpha\, \rho_{\text{buy}}(t), \quad 0 < \alpha \leq 1 \qquad (1)$$

where α denotes the selling coefficient. The hourly PV energy is obtained by scaling a base generation profile:

$$E_{\text{PV}}(t) = k_{\text{PV}}\, E_{\text{PV}}^{\text{base}}(t), \quad k_{\text{PV}} \in \{1,2,3\} \qquad (2)$$

The base profile yields 14.8 kWh per day, so the scaling factors 2 and 3 correspond to 29.6 kWh and 44.4 kWh, respectively. Table 3 and Fig. 3 present the tariff, the base PV profile and the fixed base load. The tariff peaks in hours 8–10 (0.2450–0.2735 \$/kWh), when PV output is still moderate and the fixed load reaches its morning peak, and it remains below 0.10 \$/kWh from hour 16 onwards, when the fixed load attains its evening maximum of 2.2 kWh in hour 18. This pattern favours storing low-cost night-time or midday energy and releasing it during the short morning price peak.

TABLE 3. Hourly purchase price [9], [35], base PV energy and fixed base load

Hour	1	2	3	4	5	6	7	8	9	10	11	12
Price ($/kWh)	0.1000	0.1000	0.0850	0.0900	0.1200	0.0900	0.1200	0.2450	0.2700	0.2735	0.1700	0.1650
Base PV (kWh)	0.0	0.0	0.0	0.0	0.0	0.1	0.3	0.6	0.9	1.2	1.5	1.8
Fixed load (kWh)	0.5	0.4	0.3	0.3	0.4	0.6	1.2	1.8	1.5	1.2	0.9	0.8
Hour	**13**	**14**	**15**	**16**	**17**	**18**	**19**	**20**	**21**	**22**	**23**	**24**
Price ($/kWh)	0.1650	0.1630	0.1400	0.0900	0.0850	0.0880	0.0950	0.0810	0.0820	0.0820	0.0820	0.0820
Base PV (kWh)	2.0	1.8	1.5	1.2	0.9	0.6	0.3	0.1	0.0	0.0	0.0	0.0
Fixed load (kWh)	0.9	1.0	1.1	1.3	1.8	2.2	1.8	1.4	1.0	0.8	0.6	0.5

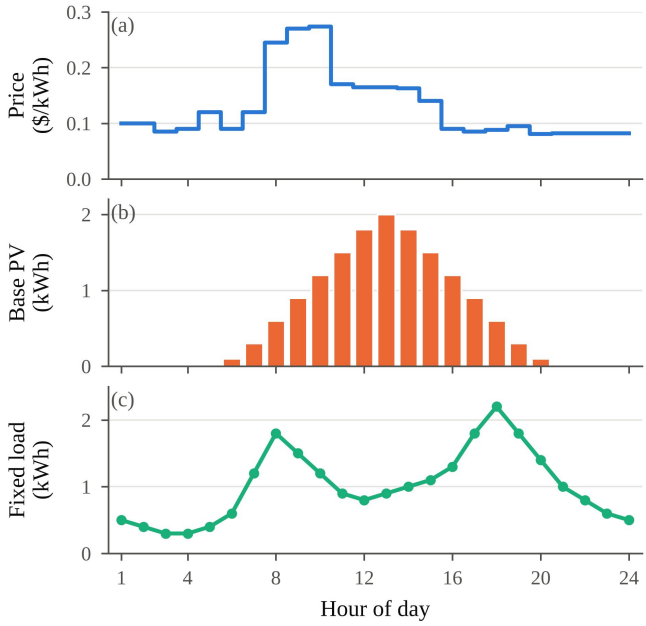


FIGURE 3. Hourly inputs of the household model: (a) purchase price, (b) base PV energy and (c) fixed base load.

C. Shiftable Appliance Model

The household demand in slot t comprises the fixed base load and the consumption of the shiftable appliances that are ON in that slot:

$$E_{\mathrm{L}}(t) = E_{\mathrm{fix}}(t) + \sum_{a \in \mathcal{A}} P_a \; x_a(t) \, \Delta t \qquad (3)$$

where $\mathcal{A} = \mathcal{A}_{\mathrm{N}} \cup \mathcal{A}_{\mathrm{I}}$. Each appliance must operate for its required number of hours:

$$\sum_{t=1}^{T} x_a(t) = h_a, \qquad \forall a \in \mathcal{A} \tag{4}$$

The dishwasher, clothes dryer and washing machine are non-interruptible; they may start in any admissible slot but must then operate continuously:

$$x_a(t) = \begin{cases} 1, & \tau_a \le t \le \tau_a + h_a - 1 \\ 0, & \text{otherwise} \end{cases} \tag{5}$$

for $a \in \mathcal{A}_{\mathrm{N}}$, with $\tau_a \in \{1, \ldots, T - h_a + 1\}$. The water heater and the air conditioner are interruptible, so their h_a operating hours may be distributed freely over the day. Table 4 lists the power ratings and operating durations, which are adopted from [9], [35]; together, the five appliances require 28.4 kWh per day. Thermal comfort dynamics and minimum ON/OFF times are not modelled.

TABLE 4. Shiftable appliances

Appliance	Type	Rated power (kW)	Hours h_a	Energy (kWh)
Dishwasher	Non-interruptible	0.2	3	0.6
Clothes dryer	Non-interruptible	0.7	4	2.8
Washing machine	Non-interruptible	0.8	5	4.0
Water heater	Interruptible	1.0	8	8.0
Air conditioner	Interruptible	1.3	10	13.0

D. Energy Storage System Model

The controller issues a single signed command $u_{\mathrm{E}}(t)$ to the ESS in each slot, where a positive value denotes a charging request and a negative value a discharging request:

$$\begin{aligned} c_{\mathrm{E}}(t) &= \max\{u_{\mathrm{E}}(t), 0\}, \\ d_{\mathrm{E}}(t) &= \max\{-u_{\mathrm{E}}(t), 0\} \end{aligned} \tag{6}$$

Since both components are derived from a single quantity, the ESS can never charge and discharge within the same slot. Each request is further limited by the rate of the ESS and by its free capacity or usable energy:

$$\hat{c}_{\mathrm{E}}(t) = \min\{c_{\mathrm{E}}(t),\, R_{\mathrm{E}},\, \bar{c}_{\mathrm{E}}(t)\}, \qquad \bar{c}_{\mathrm{E}}(t) = \frac{E_{\mathrm{E}}^{\max} - E_{\mathrm{E}}(t-1)}{\eta_{\mathrm{E}}} \tag{7}$$

$$D_{\mathrm{E}}(t) = \min\{d_{\mathrm{E}}(t),\, R_{\mathrm{E}},\, \bar{d}_{\mathrm{E}}(t)\}, \qquad \bar{d}_{\mathrm{E}}(t) = \eta_{\mathrm{E}}\left(E_{\mathrm{E}}(t-1) - E_{\mathrm{E}}^{\min}\right) \tag{8}$$

Here, $\bar{c}_{\mathrm{E}}(t)$ denotes the free capacity expressed as input energy, $\bar{d}_{\mathrm{E}}(t)$ is the energy that can be withdrawn from the ESS without depleting it below its minimum level, and $D_{\mathrm{E}}(t)$ is the energy actually delivered by the ESS in slot t. The stored energy evolves as

$$E_{\mathrm{E}}(t) = E_{\mathrm{E}}(t-1) + \eta_{\mathrm{E}}\,\hat{c}_{\mathrm{E}}(t) - \frac{D_{\mathrm{E}}(t)}{\eta_{\mathrm{E}}} \tag{9}$$

and must satisfy the operating limits and boundary conditions

$$E_{\mathrm{E}}^{\min} \le E_{\mathrm{E}}(t) \le E_{\mathrm{E}}^{\max}, \quad E_{\mathrm{E}}(0) = E_{\mathrm{E}}^{\mathrm{init}}, \quad E_{\mathrm{E}}(T) = E_{\mathrm{E}}^{\mathrm{term}} \tag{10}$$

The ESS parameters adopted in the three experimental studies described in Section V-B are listed in Table 5.

TABLE 5. Storage parameters (energies in kWh, rates in kWh/slot)

Device and study	$E^{\max}$	$E^{\min}$	E^{init}	E^{term}	R	η
ESS, benchmark household	5.0	0.5	2.5	0.5	0.9	0.95
ESS, storage study	3.0 or non-binding	0.5	0.5	0.5	0, 0.3, 0.6, 0.9	0.95
ESS, PV and selling-price study	3.0	0.5	0.5	0.5	0.3, 0.6, 0.9	0.95

Note: The non-binding capacity is 15.18 kWh at 0.6 kWh/slot and 22.02 kWh at 0.9 kWh/slot; these values are sufficiently large that the capacity limit never constrains operation within the day, which isolates the effect of the rate.

E. Hourly Energy-Flow Allocation

The hourly allocation follows a fixed priority order. PV energy is first allocated to the household load, yielding a PV surplus and a residual load:

$$\begin{aligned} E_{\mathrm{PV}}^{\mathrm{load}}(t) &= \min\{E_{\mathrm{PV}}(t), E_{\mathrm{L}}(t)\}, \\ E_{\mathrm{PV}}^{\mathrm{sur}}(t) &= E_{\mathrm{PV}}(t) - E_{\mathrm{PV}}^{\mathrm{load}}(t), \\ E_{\mathrm{L}}^{\mathrm{res}}(t) &= E_{\mathrm{L}}(t) - E_{\mathrm{PV}}^{\mathrm{load}}(t) \end{aligned} \tag{11}$$

The PV energy available for charging is limited by both the PV surplus and the feasible charging request of the ESS:

$$E_{\mathrm{PV}}^{\mathrm{ch}}(t) = \min\{E_{\mathrm{PV}}^{\mathrm{sur}}(t),\ \hat{c}_{\mathrm{E}}(t)\} \tag{12}$$

The portion of the charging request that cannot be met by PV is supplied by the grid:

$$E_{\mathrm{grid}}^{\mathrm{ch}}(t) = \hat{c}_{\mathrm{E}}(t) - E_{\mathrm{PV}}^{\mathrm{ch}}(t) \tag{13}$$

Surplus PV energy that is neither consumed nor stored is accounted for as wastage:

$$E_{\mathrm{PV}}^{\mathrm{waste}}(t) = E_{\mathrm{PV}}^{\mathrm{sur}}(t) - E_{\mathrm{PV}}^{\mathrm{ch}}(t) \tag{14}$$

Subsequently, the ESS supplies the residual load, with its contribution bounded by both the residual load and its deliverable energy:

$$E_{\mathrm{E}}^{\mathrm{load}}(t) = \min\{E_{\mathrm{L}}^{\mathrm{res}}(t),\ D_{\mathrm{E}}(t)\} \tag{15}$$

Any deliverable energy in excess of the household demand is sold to the grid:

$$E_{\mathrm{E}}^{\mathrm{sell}}(t) = D_{\mathrm{E}}(t) - E_{\mathrm{E}}^{\mathrm{load}}(t) \tag{16}$$

Finally, the grid import covers the load served by neither PV nor the ESS, together with the grid-supplied share of the charging energy:

$$E_{\mathrm{grid}}(t) = E_{\mathrm{L}}^{\mathrm{res}}(t) - E_{\mathrm{E}}^{\mathrm{load}}(t) + E_{\mathrm{grid}}^{\mathrm{ch}}(t) \tag{17}$$

Under these rules, each ESS command maps to exactly one allocation, and the simulator therefore returns a unique, well-defined schedule for every candidate.

F. Objective Function and Performance Indicators

The objective is the daily electricity cost, defined as the payment for grid imports minus the revenue from energy sold from storage [9]:

$$C_{\text{day}} = \sum_{t=1}^{T} \rho_{\text{buy}}(t)\, E_{\text{grid}}(t) - \sum_{t=1}^{T} \rho_{\text{sell}}(t)\, E_{\text{E}}^{\text{sell}}(t) \tag{18}$$

Three additional indicators characterise each schedule but are not optimised. The PAR of the grid demand [9] is given by

$$\text{PAR} = \frac{\max_t E_{\text{grid}}(t)}{\frac{1}{T}\sum_{t=1}^{T} E_{\text{grid}}(t)} \tag{19}$$

while the daily PV wastage and PV utilisation are defined as

$$W_{\text{PV}} = \sum_{t=1}^{T} E_{\text{PV}}^{\text{waste}}(t), \qquad U_{\text{PV}} = \left(1 - \frac{W_{\text{PV}}}{\sum_{t=1}^{T} E_{\text{PV}}(t)}\right) \times 100\% \tag{20}$$

These indicators reveal how a purely cost-driven schedule affects the grid and the utilisation of local generation.

G. Decision-Variable Encoding and Optimisation Problem

Each candidate schedule is represented by the continuous decision vector

$$\mathbf{z} = [s_1, s_2, s_3, \boldsymbol{\pi}_4, \boldsymbol{\pi}_5, \mathbf{u}_{\text{E}}] \tag{21}$$

where s_1, s_2 and s_3 are the start variables of the dishwasher, clothes dryer and washing machine, respectively; $\boldsymbol{\pi}_4$ and $\boldsymbol{\pi}_5$ are the 24-element priority vectors of the water heater and the air conditioner; and $\mathbf{u}_{\text{E}}$ contains the 24 hourly ESS commands, giving 75 variables in total. Each variable is confined to a fixed interval $[l_k, u_k]$: the interval of a start variable spans the admissible start slots of the corresponding appliance, whereas that of a storage command is bounded by the rate of the ESS. A start variable is decoded by rounding and clipping,

$$\tau_a = \min\{\max\{\text{round}(s_a), 1\}, T - h_a + 1\} \tag{22}$$

after which (5) generates the contiguous operating block. An interruptible appliance operates in the h_a slots with the highest priority scores:

$$x_a(t) = \begin{cases} 1, & t \in \Omega_a \\ 0, & \text{otherwise} \end{cases}, \qquad \Omega_a = \underset{\Omega \subset \{1,\ldots,T\},\, |\Omega| = h_a}{\text{argmax}} \sum_{t \in \Omega} \pi_a(t) \tag{23}$$

With this encoding, 51 continuous appliance variables replace the 120 binary ON/OFF decisions of a direct formulation, and every decoded schedule inherently satisfies (4) and (5). The optimisation problem is then stated as

$$\min_{\mathbf{z} \in [\mathbf{l}, \mathbf{u}]} C_{\text{day}}(\mathbf{z}) \quad \text{subject to (3)–(17)} \tag{24}$$

The rate and capacity limits in (7)–(9) are enforced by the simulator, and the violation of the terminal condition in (10) is quantified by

$$V(\mathbf{z}) = |E_{\mathrm{E}}(T) - E_{\mathrm{E}}^{\mathrm{term}}| \qquad (25)$$

During the search, all algorithms minimise the penalised cost

$$\widetilde{C}(\mathbf{z}) = C_{\mathrm{day}}(\mathbf{z}) + \Psi\big(V(\mathbf{z})\big) \qquad (26)$$

where the penalty Ψ is zero for $V(\mathbf{z}) = 0$ and positive otherwise. A run is regarded as feasible only if its final best vector satisfies $V(\mathbf{z}^*) = 0$, and only feasible runs are included in the reported statistics. Since all five algorithms share the same encoding, simulator and objective, any differences in their results are attributable solely to their search strategies.

Proposed Hybrid Quantum Differential Evolution Algorithm

HQDE builds on classic DE [12] and incorporates four additional components: current-to-p-best mutation with generation-dependent control parameters, inspired by adaptive DE [38]; a quantum-inspired angle-space update restricted to the appliance variables [16], [17]; a best-guided search phase in the later stage of the run; and a stagnation-recovery mechanism. Fig. 4 illustrates the integration of HQDE within the HEMS controller.

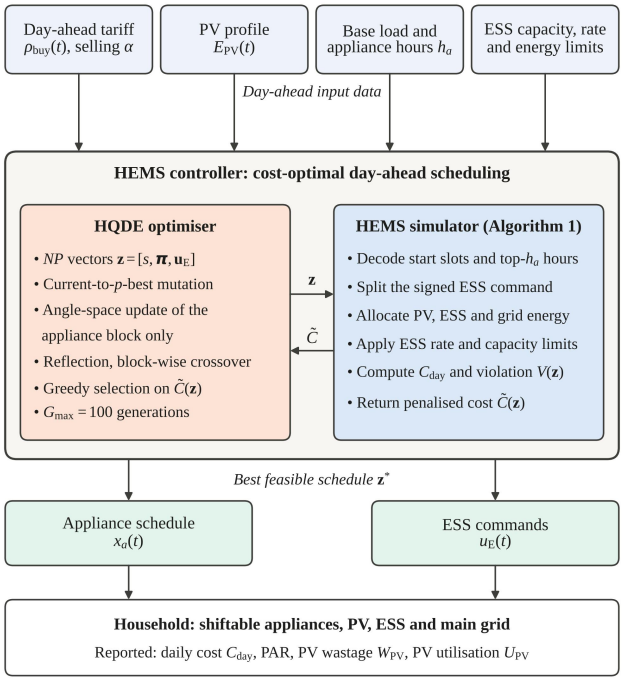


FIGURE 4. HQDE-based HEMS framework for cost-optimal day-ahead scheduling.

A. Rationale for Differentiated Treatment of the Decision Variables

The storage commands in (21) represent physical energies, so a small change in $u_{\mathrm{E}}(t)$ alters the dispatch, the stored energy and the cost smoothly. In contrast, the appliance variables affect the schedule only through rounding (22) and ranking (23). A start variable can change by almost one unit without altering the schedule, and the priority scores are relevant only through their relative order;

consequently, the cost is a piecewise-constant function of these variables with extensive plateaus. Difference vectors computed on such plateaus are frequently too small to modify the decoded schedule. HQDE therefore provides the appliance block with an additional, nonlinearly scaled search direction through an angle representation, whereas the storage commands are retained in the real domain, where differential steps preserve their physical meaning.

B. Current-to-p-best Mutation with Scheduled Control Parameters

For each target vector $\mathbf{x}_i$, a guide $\mathbf{x}_{\text{pbest}}$ is selected at random from the best $[p\,NP]$ vectors, and two further mutually distinct vectors $\mathbf{x}_{r_1}$ and $\mathbf{x}_{r_2}$, both different from $\mathbf{x}_i$, are drawn from the population. The real-domain mutant vector is then generated as

$$\mathbf{v}_i^R = \mathbf{x}_i + F_i\big(\mathbf{x}_{\text{pbest}} - \mathbf{x}_i\big) + F_i\big(\mathbf{x}_{r_1} - \mathbf{x}_{r_2}\big) \tag{27}$$

The first difference term drives the target towards a promising region, whereas the second introduces variation drawn from the population. Each candidate samples its own F_i and CR_i around mean values that follow predefined schedules over the run: the mean scale factor μ_F decreases from 0.78 to 0.42, the mean crossover rate μ_{CR} increases from 0.80 to 0.98, and the elite fraction p decreases from 0.20 to 0.04. Consequently, early generations take large steps guided by a broad elite, whereas later generations take small steps guided by the very best vectors. Unlike JADE [38] and SHADE [39], HQDE does not learn its parameters from successful values and maintains no external archive.

C. Quantum-Inspired Angle-Space Update of the Appliance Block

Each appliance variable x_k with bounds $[l_k, u_k]$ is first normalised,

$$\zeta_k = \frac{x_k - l_k}{u_k - l_k} \tag{28}$$

and then mapped to an angle,

$$\theta_k = \arcsin\big(\sqrt{\zeta_k}\big), \qquad 0 \le \theta_k \le \frac{\pi}{2} \tag{29}$$

which is transformed back to the variable domain by

$$x_k^Q = l_k + (u_k - l_k)\sin^2\theta_k \tag{30}$$

The quantity $\sin^2\theta_k$ therefore plays the role of the probability amplitude of a qubit [16]. In the angle space, the appliance block of candidate i is mutated through a differential term and an attraction towards the p-best guide,

$$\boldsymbol{\theta}_i^M = \boldsymbol{\theta}_i + F_i\big(\boldsymbol{\theta}_{r_1} - \boldsymbol{\theta}_{r_2}\big) + \lambda\big(\boldsymbol{\theta}_{\text{pbest}} - \boldsymbol{\theta}_i\big) \tag{31}$$

where the attraction strength λ increases from 0.55 to 1.00 over the run. The mutated angles are reflected into $[0, \pi/2]$ and transformed back using (30), yielding the quantum-derived candidate $\mathbf{x}_i^Q$. Owing to the nonlinearity of the sine-squared mapping, equal angle steps produce larger moves near the centre of the variable range than near its bounds, thereby providing the appliance block with a search direction distinct from that of the real-domain mutant. The two mutants are combined as follows:

$$\mathbf{v}_i^{\mathcal{A}} = [1 - q(g)]\mathbf{v}_i^{R,\mathcal{A}} + q(g)\,\mathbf{x}_i^{Q} \qquad (32)$$

where $\mathbf{v}_i^{R,\mathcal{A}}$ denotes the appliance block of (27). The weight $q(g)$ decreases from 0.35 to 0.06, so that the angle-space direction is most influential early in the run, when diversity is most important, and gradually diminishes as the search shifts towards refinement. The ESS component of the mutant is taken directly from (27).

D. Best-Guided Search and Stagnation Recovery

Once 55% of the generation budget has been consumed, the real-domain mutation is centred more strongly on the current best vector, thereby concentrating the remaining evaluations around the most promising schedule. Independently of this phase, each candidate maintains a counter of consecutive generations without improvement. When this counter reaches six, the next mutation of that candidate is centred on the best vector, and a small perturbation is applied to its appliance angles to enable it to escape the plateau on which it has stagnated.

E. Boundary Handling, Crossover and Selection

Components that violate their bounds are folded back into the feasible interval by periodic reflection. For a component y with bounds $[l, u]$ and width $\Delta = u - l$,

$$y' = \begin{cases} l + m, & m \le \Delta \\ l + 2\Delta - m, & m > \Delta \end{cases}, \qquad m = (y - l) \bmod 2\Delta \qquad (33)$$

and the same rule confines the angles to $[0, \pi/2]$. Binomial crossover then generates the trial vector,

$$t_{i,k} = \begin{cases} v_{i,k}, & r_{i,k} \le CR_i \text{ or } k \in \mathcal{K}_i \\ x_{i,k}, & \text{otherwise} \end{cases} \qquad (34)$$

where $r_{i,k}$ is uniformly distributed in [0,1] and $\mathcal{K}_i$ contains one randomly selected index from each active block (appliance and ESS), which ensures that every block of the trial vector inherits at least one component from the mutant. After decoding and evaluation, the trial vector replaces its parent if it is not inferior:

$$\mathbf{x}_i^{(g+1)} = \begin{cases} \mathbf{t}_i, & \widetilde{C}(\mathbf{t}_i) \le \widetilde{C}\left(\mathbf{x}_i^{(g)}\right) \\ \mathbf{x}_i^{(g)}, & \text{otherwise} \end{cases} \qquad (35)$$

where $\widetilde{C}$ denotes the penalised cost defined in (26).

F. Algorithmic Procedure and Computational Complexity

Algorithm 1 details the evaluation of a candidate solution, while Algorithm 2 and Fig. 5 summarise the complete HQDE procedure.

Algorithm 1. Evaluation of a candidate schedule
Input: decision vector **z**; household and storage data (Tables 3–5)

Output: penalised cost $\widetilde{C}$; C_{day}, PAR, W_{PV}, U_{PV}; decoded schedule
1: **for** each $a \in \mathcal{A}_{\mathrm{N}}$: obtain τ_a by (22) and $x_a(t)$ by (5)
2: **for** each $a \in \mathcal{A}_{\mathrm{I}}$: obtain $x_a(t)$ by (23)
3: form $E_{\mathrm{L}}(t)$ by (3); set $E_{\mathrm{E}}(0) = E_{\mathrm{E}}^{\mathrm{init}}$
4: **for** $t = 1$ to T **do**
5: split $u_{\mathrm{E}}(t)$ by (6) and limit the requests by (7) and (8)
6:assign PV energy to load, charging and wastage by (11)–(14)
7:assign ESS discharge to load and sales by (15) and (16)
8: update $E_{\mathrm{E}}(t)$ by (9)
9: obtain $E_{\mathrm{grid}}(t)$ by (17)
10: **end for**
11: compute C_{day} by (18) and PAR, W_{PV}, U_{PV} by (19) and (20)
12: compute $V(\mathbf{z})$ by (25) and $\widetilde{C}$ by (26)
13: **return** $\widetilde{C}$, the indicators and the schedule

Algorithm 2. HQDE for cost-optimal 24-hour HEMS scheduling

Input: NP, $G_{\max}$, bounds $[\mathbf{l}, \mathbf{u}]$, parameter schedules (Table 8)
Output: best feasible decision vector $\mathbf{z}^*$ and its decoded schedule
1: **initialise** NP vectors uniformly in $[\mathbf{l}, \mathbf{u}]$ and evaluate each by Algorithm 1
2:convert the appliance block of each vector to angles by (28) and (29); set all stagnation counts to zero
3: **for** $g = 1$ to $G_{\max}$ **do**
4: rank the population; update μ_F, μ_{CR}, p, λ and $q(g)$
5: **for** $i = 1$ to NP **do**
6: draw F_i and CR_i; choose $\mathbf{x}_{\mathrm{pbest}}$, $\mathbf{x}_{r_1}$ and $\mathbf{x}_{r_2}$
7: form $\mathbf{v}_i^R$ by (27), in best-guided or recovery mode when active (Section IV-D)
8: form $\boldsymbol{\theta}_i^M$ by (31), reflect it and map it back by (30)
9:blend the appliance block by (32); copy the ESS block of $\mathbf{v}_i^R$
10:apply (33) and build $\mathbf{t}_i$ by (34)
11: evaluate $\mathbf{t}_i$ by Algorithm 1
12:select by (35); reset the count of i on acceptance, otherwise increase it
13: **end for**
14: **end for**
15: **return** the best feasible $\mathbf{z}^*$ and its schedule

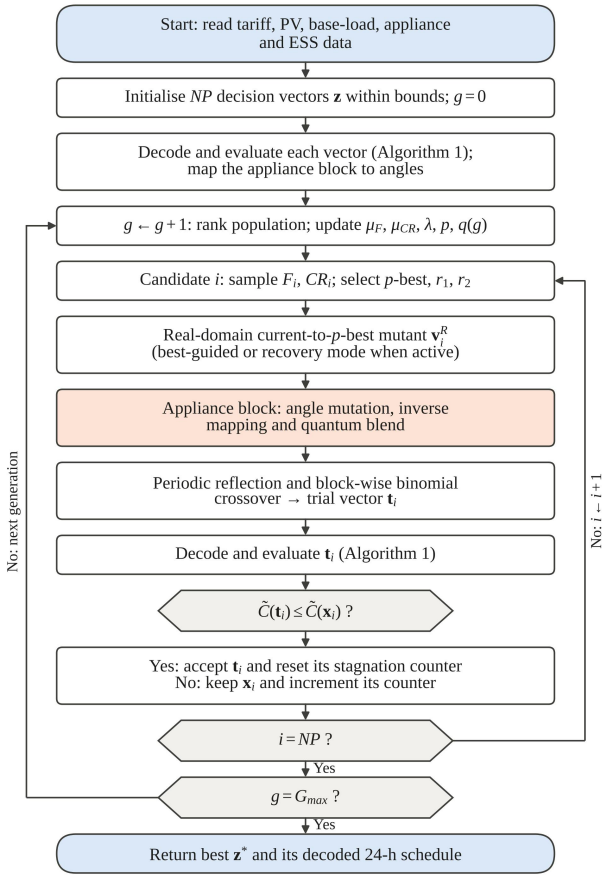


FIGURE 5. Flowchart of HQDE for cost-optimal HEMS scheduling.

A single run requires $NP(G_{\max}+1)$ fitness evaluations, i.e., 5050 evaluations for $NP = 50$ and $G_{\max} = 100$. Decoding sorts the priority scores in $O(T\log T)$ time and simulates the day in $O(T|\mathcal{A}|)$ time, while the variation operators require $O(D)$ operations per candidate, where $D = 75$ is the problem dimension. Including the ranking of the population in each generation, the overall complexity of one run is $O(G_{\max} NP\,(D + T\log T) + G_{\max} NP\log NP)$. Relative to standard DE, the angle mapping affects only the constant factor, and the evaluation budget is identical for all compared methods.

Experimental Setup

A. Input Data and Parameter Sources

The hourly tariff in Table 3 and the appliance data in Table 4 are taken from the household inputs of Dinh et al. [9] and Ahmad et al. [35]. The base PV profile and the fixed base load are listed in Table 3, and the ESS settings of the benchmark household, in which the ESS begins the day with 2.5 kWh, are given in Table 5. In the storage and PV studies, the ESS has a minimum and initial energy of 0.5 kWh and an efficiency of 0.95, with a capacity of 3 kWh unless a non-binding capacity is specified (Table 5). Because the ESS begins the day with less stored energy in these two studies, their costs should not be compared

directly with those of the benchmark household. All data required to reproduce the experiments are provided in Tables 3–5.

B. Design of the Experimental Studies

The experiments are organised into three studies, each designed to address a specific research question (Table 6). The benchmark household, with base PV, $\alpha = 1.0$ and a 5 kWh ESS rated at 0.9 kWh/slot, is used to rank the five algorithms. The storage study examines how the capacity and charge/discharge rate of the ESS affect the minimum cost, using base PV, $\alpha = 0.9$ and six storage configurations. The PV and selling-price study investigates the interaction between PV size, selling coefficient and ESS rate by combining two PV sizes, three selling coefficients and three rates of a 3 kWh ESS into 18 configurations. In all studies, the daily cost (18) is the sole objective.

TABLE 6. Experimental studies

Study	PV	α	ESS	Evaluation
Benchmark household	1×	1.0	5 kWh, 0.9 kWh/slot	50 runs per algorithm
Storage study	1×	0.9	None, 3 kWh or non-binding; 0–0.9 kWh/slot	6 configurations; 50 runs
PV and selling-price study	2×, 3×	1.0, 0.9, 0.8	3 kWh; 0.3, 0.6, 0.9 kWh/slot	18 configurations; best HQDE solution

C. Benchmark Algorithms and Comparison Protocol

HQDE is compared with four algorithms representing the principal algorithm families employed in HEMS research (Table 7): a GA [10], [24]; the PSO+BPSO hybrid of Dinh et al. [9]; standard DE [12], on which HQDE is based; and the IDE of Essiet et al. [13], the closest DE-based smart-home study. All methods employ the evaluation procedure of Algorithm 1, identical bounds and input data, a population size of 50 and a budget of 100 generations. Each repeated-run experiment comprises 50 independent runs per method with different random seeds. The HQDE settings are listed in Table 8.

TABLE 7. Compared algorithms

Algorithm	Search mechanism	Basis
GA	Selection, crossover and mutation of a population of schedules	[10], [24]
PSO+BPSO	Particle search over continuous and binary scheduling variables	[9], [25]
DE	Differential mutation, binomial crossover and greedy replacement	[12]
IDE	Improved DE for smart-home energy management	[13]
HQDE	Current-to-p-best DE with scheduled parameters and quantum-inspired appliance update	This work; [16], [38]

TABLE 8. HQDE settings

Setting	Value
Population size NP	50
Generation budget $G_{\max}$	100
Mean scale factor μ_F	0.78 → 0.42
Mean crossover rate μ_{CR}	0.80 → 0.98
Elite fraction p	0.20 → 0.04
Angle-space attraction λ	0.55 → 1.00
Quantum blend weight $q(g)$	0.35 → 0.06
Start of best-guided search	After 55% of $G_{\max}$
Stagnation threshold	6 generations
Boundary handling	Periodic reflection (33)
Crossover	Binomial with block participation (34)
Selection	One-to-one greedy (35)

D. Performance Metrics

For each repeated-run experiment, the best, worst, mean and median values and the standard deviation of the daily cost are reported, together with the number of feasible runs. The improvement of HQDE over a reference method is expressed as the relative reduction in a statistic m:

$$\Delta_m = \frac{m_{\text{ref}} - m_{\text{HQDE}}}{m_{\text{ref}}} \times 100\% \qquad (36)$$

A positive Δ_m indicates that HQDE achieves the lower, and hence better, value.

Results and Discussion

This section presents the results of the three studies in turn and subsequently discusses the robustness of the algorithms, the comparison with related work and the practical implications. Since the daily cost is the sole objective, PAR, PV wastage and PV utilisation are reported as descriptive indicators only.

A. Comparative Performance on the Benchmark Household

Table 9 summarises the results of 50 runs of each algorithm on the benchmark household. HQDE attains the lowest best ($2.5213), mean ($2.6023) and worst ($2.7344) costs. IDE ranks second; relative to IDE, HQDE reduces the best cost by 10.21%, the mean cost by 9.75% and the worst cost by 7.81%. The standard deviation of HQDE (0.0304) is approximately 10% lower than that of IDE (0.0338), indicating that the cost reduction is achieved with lower run-to-run variability. Compared with DE, GA and PSO+BPSO, the mean cost is reduced by 12.03%, 12.24% and 30.46%, respectively. Notably, even the worst HQDE run is cheaper than the best run of every other method; that is, the least successful HQDE run outperformed the best of the 50 runs of each baseline.

TABLE 9. Daily cost on the benchmark household over 50 runs ($)

Algorithm	Best	Worst	Mean	Std. dev.
HQDE	**2.5213**	**2.7344**	**2.6023**	**0.0304**
IDE	2.8081	2.9659	2.8834	0.0338
DE	2.8866	3.0565	2.9580	0.0343
GA	2.8684	3.1880	2.9653	0.0588
PSO+BPSO	3.1478	4.2364	3.7419	0.2621

Fig. 6 depicts the convergence of the best run of each method. IDE descends most rapidly in the initial generations, but HQDE overtakes it at approximately generation 28 and continues to improve until it stabilises near $2.52, whereas IDE settles near $2.81. GA and DE stagnate between $2.86 and $2.89, and PSO+BPSO stagnates near $3.15. This behaviour is consistent with the design of HQDE: large early steps and the angle-space update maintain population diversity in the initial phase, and the progressively narrowing p-best guidance and the best-guided phase in later generations subsequently convert this diversity into a lower final cost.

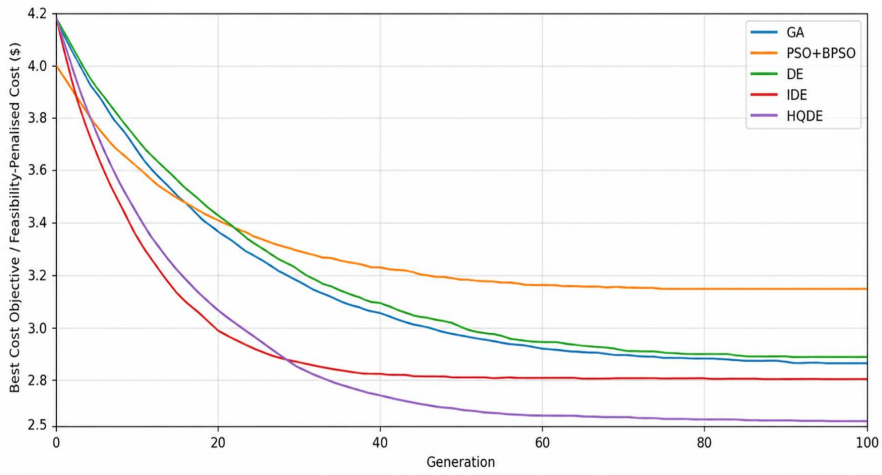


FIGURE 6. Convergence of the best run of each algorithm on the benchmark household (best penalised daily cost per generation).

The best HQDE schedule exhibits a PAR of 3.0111, wastes 0.3000 kWh of PV energy and utilises 97.973% of the PV output. Although these indicators were not optimised, they demonstrate that, with base PV and a 5 kWh ESS, a cost-driven schedule already absorbs almost the entire PV generation.

B. Effect of ESS Capacity and Charge/Discharge Rate

Table 10 reports the results for the six storage configurations. The minimum cost denotes the lowest single-run cost obtained for each configuration, the best-run column identifies the method that achieved it, and the gain is the value of Δ_m for the HQDE mean cost relative to the IDE mean over 50 runs. Fig. 7(a) shows the minimum costs, and Fig. 7(b) shows the mean costs of the two methods.

TABLE 10. Storage study: minimum cost and mean cost over 50 runs

ESS capacity	Rate	Best run	Min. cost ($)	IDE mean ($)	HQDE mean ($)	Gain (%)
No ESS	0	HQDE	3.6246	3.6618	3.6439	0.4877
3 kWh	0.3	HQDE	3.4344	3.5022	3.4731	0.8309
3 kWh	0.6	HQDE	3.2463	3.3515	3.2985	1.5797
Non-binding	0.6	IDE	3.2376	3.3233	3.2939	0.8833
3 kWh	0.9	HQDE	3.1533	3.2494	3.2154	1.0446
Non-binding	0.9	HQDE	3.0711	3.1634	3.1353	0.8877

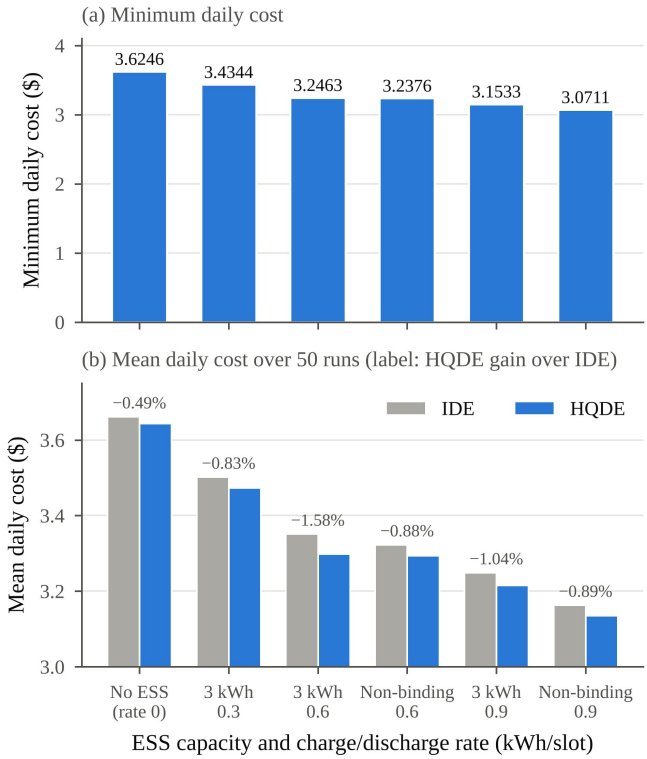


FIGURE 7. Storage study: (a) minimum daily cost for each ESS capacity and rate and (b) mean daily cost of IDE and HQDE over 50 runs.

The inclusion of storage reduces the minimum cost from $3.6246 without an ESS to $3.0711 with a non-binding capacity and a rate of 0.9 kWh/slot, corresponding to a reduction of 15.27%. The origin of this benefit is particularly informative. With the capacity fixed at 3 kWh, increasing the rate from 0.3 to 0.9 kWh/slot lowers the minimum cost by 8.18%, whereas removing the capacity limit lowers it by only 0.27% at 0.6 kWh/slot and by 2.61% at 0.9 kWh/slot. Under this tariff, the high-price period is short (hours 8–10); hence, the achievable saving is constrained by the amount of energy that the ESS can release within these few hours rather than by the amount it can store, and a faster ESS also absorbs more low-cost energy per hour. For a household exposed to a short price peak, a higher charge/discharge rating is therefore more valuable than additional capacity.

HQDE achieves a lower mean cost than IDE in all six configurations, with gains ranging from 0.49% to 1.58%; the largest gain is observed for the 3 kWh ESS at

0.6 kWh/slot. HQDE also finds the lowest-cost single schedule in five configurations. The exception is the non-binding ESS at 0.6 kWh/slot, where IDE finds the cheapest schedule while HQDE still retains the lower mean cost. The gains are smaller than those for the benchmark household, but they are consistently positive across all configurations.

C. Combined Effect of PV Size, Selling Coefficient and ESS Rate

Table 11 lists the best HQDE schedule for each of the 18 configurations, and Fig. 8 plots the daily cost against the ESS rate for each selling coefficient.

TABLE 11. PV and selling-price study: best HQDE solution for each configuration

PV	α	Rate (kWh/slot)	Cost ($)	PAR	PV waste (kWh)
2×	1.0	0.3	1.9462	3.4346	0.1056
2×	1.0	0.6	1.7488	3.6411	0.4365
2×	1.0	0.9	1.6199	3.6238	0.5019
2×	0.9	0.3	1.9776	3.8009	0.0010
2×	0.9	0.6	1.8137	3.9583	0.5012
2×	0.9	0.9	1.7136	3.1562	0.6016
2×	0.8	0.3	1.9788	3.4559	0.1009
2×	0.8	0.6	1.8631	4.0876	0.1010
2×	0.8	0.9	1.7910	3.8358	0.2044
3×	1.0	0.3	0.7194	4.8371	1.8007
3×	1.0	0.6	0.4898	4.4817	1.3022
3×	1.0	0.9	**0.3469**	4.1741	1.0011
3×	0.9	0.3	0.7762	4.4347	2.0060
3×	0.9	0.6	0.5535	4.4959	1.2105
3×	0.9	0.9	0.4496	4.3841	0.6031
3×	0.8	0.3	0.7793	4.4794	1.6015
3×	0.8	0.6	0.6381	3.9038	1.3068
3×	0.8	0.9	0.5062	3.5857	1.0003

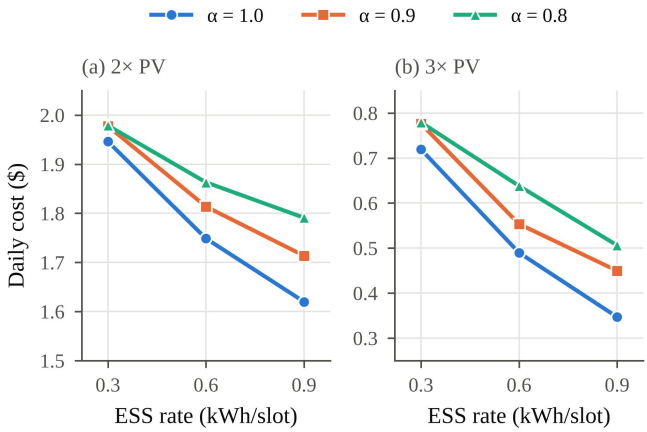


FIGURE 8. PV and selling-price study: best daily cost against ESS rate for each selling coefficient with (a) 2× PV and (b) 3× PV.

PV size is the dominant factor. For every combination of α and rate, the 3× array yields a lower cost than the 2× array; at $\alpha = 1.0$ and 0.9 kWh/slot, the cost decreases by 78.59%, from $1.6199 to $0.3469, the lowest value obtained in this

study. The ESS rate has the second-largest effect. Increasing it from 0.3 to 0.9 kWh/slot at $\alpha = 1.0$ reduces the cost by 16.77% with 2× PV and by 51.78% with 3× PV, indicating that the rate is more influential when PV is abundant, as a faster ESS can store a larger share of the midday surplus. The selling coefficient likewise becomes influential mainly when PV is abundant. At 0.9 kWh/slot, decreasing α from 1.0 to 0.8 increases the cost by 10.56% with 2× PV but by 45.92% with 3× PV, because a larger amount of stored energy is then sold and its value depends directly on α.

The indicators reveal the limitations of cost-only scheduling. The lowest-cost configuration has a PAR of 4.1741, among the highest values in the table, and with 3× PV, between 0.60 and 2.01 kWh of PV energy is wasted because the household load and the 3 kWh ESS cannot absorb the entire midday surplus. With 2× PV, the wastage does not exceed 0.61 kWh. The configuration with 2× PV, $\alpha = 0.9$ and 0.6 kWh/slot incurs a cost of \$1.8137, exhibits a PAR of 3.9583 and utilises 98.31% of the PV energy.

D. Robustness Across Independent Runs

Fig. 9 presents the mean and standard deviation of the 50-run results on the benchmark household, and Table 12 compiles the reductions in mean cost achieved by HQDE. HQDE yields the lowest mean cost among the five algorithms on the benchmark household and a lower mean cost than IDE in all six storage configurations. Its margin over IDE is 9.75% for the benchmark household and ranges from 0.49% to 1.58% across the storage configurations. PSO+BPSO exhibits by far the largest dispersion of the five methods, with a standard deviation of 0.2621, compared with 0.0304 for HQDE.

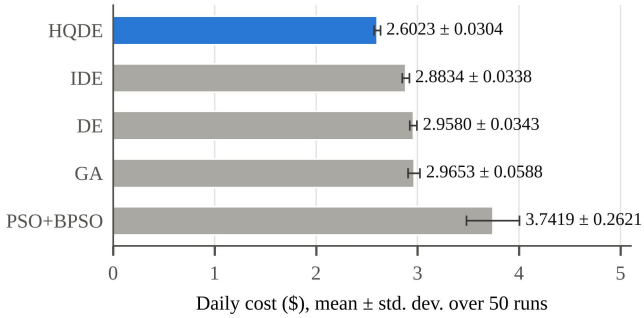


FIGURE 9. Mean and standard deviation of the daily cost over 50 runs on the benchmark household.

TABLE 12. Reduction in mean daily cost achieved by HQDE, Δ_m in (36) (%)

Experiment	vs IDE	vs GA	vs DE	vs PSO+BPSO
Benchmark household	9.75	12.24	12.03	30.46
Storage study (six configurations)	0.49–1.58	–	–	–

E. Comparison with Closely Related Studies

Table 13 positions HQDE relative to the two most closely related studies. The PSO+BPSO baseline, the PV–ESS model with energy selling, and the tariff and appliance data originate from Dinh et al. [9], whereas the IDE baseline is drawn from Essiet et al. [13]. Because the published results of these studies were

obtained with different models and settings, their reported costs are not compared directly; instead, their algorithms were executed on the simulator developed in this paper with the same evaluation budget. Under these identical conditions, the mean daily cost of HQDE on the benchmark household is 9.75% lower than that of IDE and 30.46% lower than that of PSO+BPSO.

TABLE 13. Comparison with the closest related studies

Feature	Dinh et al. [9]	Essiet et al. [13]	This work
Optimiser	PSO+BPSO	IDE	HQDE
Role in this paper	Baseline algorithm; source of tariff and appliance data	Baseline algorithm	Proposed method
Mean cost, benchmark household ($)	3.7419	2.8834	**2.6023**

Note: The mean costs were obtained by executing each algorithm on the simulator developed in this paper; the published results of the cited studies were based on different models and data and are therefore not compared directly.

Three features distinguish this work from the compared studies. First, quantum-inspired guidance is confined to the appliance block and never alters the physical ESS commands. Second, every candidate decodes into a schedule that inherently satisfies the appliance requirements. Third, the individual effects of ESS capacity, ESS rate, PV size and selling price on the minimum cost are disentangled within a single study.

F. Practical Implications and Limitations

Several practical implications emerge from the results. For a household exposed to a short and pronounced price peak, a higher ESS charge/discharge rating yields greater savings than additional capacity. PV size is the most influential determinant of the electricity bill, and the selling coefficient becomes important once PV generation is abundant, because a larger share of stored energy is then exported. However, cost-only scheduling produced PAR values between 3.01 and 4.84 in the reported best schedules and, with 3× PV, left up to 2.01 kWh of PV energy unused; households or utilities concerned with demand peaks or self-consumption therefore require criteria beyond the daily cost.

This study is subject to certain limitations. All inputs (tariff, PV output and base load) are assumed to be known one day ahead; consequently, the impact of forecast errors is not examined. Interruptible appliances are characterised solely by their rated power and daily operating time, without a thermal comfort model or minimum ON/OFF times. The results pertain to a single household and a single set of profiles. No statistical significance test was performed on the 50-run samples, and the HQDE parameter schedules were selected for this problem rather than derived through systematic tuning. Furthermore, computation times were not compared, although all methods used the same number of evaluations.

Conclusions and Future Work

This paper has presented HQDE, a hybrid quantum differential evolution algorithm for the cost-optimal day-ahead scheduling of a smart home equipped with shiftable appliances, rooftop PV and a stationary ESS. The search mechanism combines elite-guided differential mutation and generation-dependent parameter schedules with a qubit-amplitude-inspired angle-space update applied exclusively to the appliance variables. Every candidate is decoded into a schedule that satisfies the appliance operating-hour requirements, and a fixed allocation order coordinates PV generation, ESS operation and grid exchange in every hour.

In 50-run comparisons on a common simulator, HQDE achieved the lowest mean daily cost among the five algorithms. It reduced the mean cost of IDE, the strongest baseline, by 9.75% for the benchmark household and maintained a lower mean cost than IDE in all six storage configurations; moreover, on the benchmark household, even its worst run was cheaper than the best run of every baseline. The sensitivity analyses demonstrated that PV size has the strongest influence on cost, that the ESS rate is more important than its capacity under a short price peak, and that the selling coefficient becomes influential when PV generation is abundant.

Future research will be pursued in four directions. First, a plug-in electric vehicle will be incorporated into the household model as a mobile storage resource that is available only while parked at home and must satisfy its departure, arrival and end-of-day energy requirements. Second, the problem will be extended to a multi-objective formulation that minimises the daily cost together with PAR and PV wastage, since cost-only schedules were found to produce high demand peaks and, under abundant PV, unused generation. Third, uncertainty in prices, PV output and load will be addressed through stochastic or robust scheduling coupled with short-term load forecasting, and thermal comfort models and minimum ON/OFF times will be introduced for the water heater and the air conditioner. Fourth, the algorithmic evaluation will be strengthened through statistical significance testing, systematic parameter tuning and comparison with additional recent metaheuristics, and the approach will be extended from a single household to communities with shared storage.

Declarations

Conflict of interest: The authors declare that they have no conflict of interest.

Data availability: All input data used in this study are reported in Tables 3–5, and their sources are specified in Section V-A.

References

[1] A. Joseph and P. Balachandra, “Smart grid to energy internet: A systematic review of transitioning electricity systems,” IEEE Access, vol. 8, pp. 215787–215805, 2020, doi: 10.1109/ACCESS.2020.3041031.

[2] P. Palensky and D. Dietrich, “Demand side management: Demand response, intelligent energy systems, and smart loads,” IEEE Trans. Ind. Informat., vol. 7, no. 3, pp. 381–388, 2011, doi: 10.1109/TII.2011.2158841.

[3] A.-H. Mohsenian-Rad, V. W. S. Wong, J. Jatskevich, R. Schober, and A. Leon-

Garcia, “Autonomous demand-side management based on game-theoretic energy consumption scheduling for the future smart grid,” IEEE Trans. Smart Grid, vol. 1, no. 3, pp. 320–331, 2010.

[4] H. Shareef, M. S. Ahmed, A. Mohamed, and E. Al Hassan, “Review on home energy management system considering demand responses, smart technologies, and intelligent controllers,” IEEE Access, vol. 6, pp. 24498–24509, 2018.

[5] S. Panda et al., “Residential demand side management model, optimization and future perspective: A review,” Energy Rep., vol. 8, pp. 3727–3766, 2022.

[6] N. Javaid, G. Hafeez, S. Iqbal, N. Alrajeh, M. S. Alabed, and M. Guizani, “Energy efficient integration of renewable energy sources in the smart grid for demand side management,” IEEE Access, vol. 6, pp. 77077–77096, 2018.

[7] Y. Zhang, T. Ma, and H. Yang, “A review on capacity sizing and operation strategy of grid-connected photovoltaic battery systems,” Energy Built Environ., vol. 5, no. 4, pp. 500–516, 2024.

[8] J. Ma, H. H. Chen, L. Song, and Y. Li, “Residential load scheduling in smart grid: A cost efficiency perspective,” IEEE Trans. Smart Grid, vol. 7, no. 2, pp. 771–784, 2016.

[9] H. T. Dinh, J. Yun, D. M. Kim, K.-H. Lee, and D. Kim, “A home energy management system with renewable energy and energy storage utilizing main grid and electricity selling,” IEEE Access, vol. 8, pp. 49436–49450, 2020, doi: 10.1109/ACCESS.2020.2979189.

[10] A. Al-Duais, M. Osman, M. H. Shullar, and M. A. Abido, “Optimal real-time pricing-based scheduling in home energy management system using genetic algorithms,” in Proc. IEEE 4th Int. Conf. Renew. Energy Power Eng. (REPE), 2021, pp. 243–248.

[11] J.-C. Chang and T.-H. Wu, “Demand side management of power for time-of-use pricing based on particle swarm optimization,” in Proc. 3rd IEEE Int. Conf. Knowl. Innov. Invention (ICKII), 2020, pp. 317–320.

[12] R. Storn and K. Price, “Differential evolution – A simple and efficient heuristic for global optimization over continuous spaces,” J. Global Optim., vol. 11, no. 4, pp. 341–359, 1997.

[13] I. O. Essiet, Y. Sun, and Z. Wang, “Optimized energy consumption model for smart home using improved differential evolution algorithm,” Energy, vol. 172, pp. 354–365, 2019, doi: 10.1016/j.energy.2019.01.137.

[14] S. Das and P. N. Suganthan, “Differential evolution: A survey of the state-of-the-art,” IEEE Trans. Evol. Comput., vol. 15, no. 1, pp. 4–31, 2011.

[15] S. Das, S. S. Mullick, and P. N. Suganthan, “Recent advances in differential evolution – An updated survey,” Swarm Evol. Comput., vol. 27, pp. 1–30, 2016.

[16] K.-H. Han and J.-H. Kim, “Quantum-inspired evolutionary algorithm for a class of combinatorial optimization,” IEEE Trans. Evol. Comput., vol. 6, no. 6, pp. 580–593, 2002.

[17] G. Zhang, “Quantum-inspired evolutionary algorithms: A survey and empirical study,” J. Heuristics, vol. 17, no. 3, pp. 303–351, 2011.

[18] F. E. Aliabadi, K. Agbossou, S. Kelouwani, N. Henao, and S. S. Hosseini, “Coordination of smart home energy management systems in neighborhood areas: A systematic review,” IEEE Access, vol. 9, pp. 36417–36443, 2021.

[19] M. B. Rasheed et al., “Real time information based energy management using

customer preferences and dynamic pricing in smart homes," Energies, vol. 9, no. 7, p. 542, 2016, doi: 10.3390/en9070542.

[20] J. T. Flores, W. C. Celeste, D. J. C. Coura, S. das Dores Rissino, H. R. O. Rocha, and R. E. N. Moraes, "Demand planning in smart homes," IEEE Latin Am. Trans., vol. 14, no. 7, pp. 3247–3255, 2016.

[21] A. Jamil et al., "An innovative home energy management model with coordination among appliances using game theory," Sustainability, vol. 11, no. 22, p. 6287, 2019.

[22] Z. Iqbal et al., "A domestic microgrid with optimized home energy management system," Energies, vol. 11, no. 4, p. 1002, 2018.

[23] B. Xiong et al., "Hybrid robust-stochastic optimal scheduling for multi-objective home energy management with the consideration of uncertainties," Energy, vol. 290, p. 130047, 2024, doi: 10.1016/j.energy.2023.130047.

[24] Z. Irshad, S. M. H. Aejaz, U. Mustafa, A. M. F. Durrani, and F. Hafeez, "User-friendly demand side management for smart grid network," in Proc. Int. Conf. Eng. Emerg. Technol. (ICEET), 2020, pp. 1–12.

[25] J. Kennedy and R. Eberhart, "Particle swarm optimization," in Proc. IEEE Int. Conf. Neural Netw. (ICNN), 1995, vol. 4, pp. 1942–1948.

[26] S. Rahim et al., "Exploiting heuristic algorithms to efficiently utilize energy management controllers with renewable energy sources," Energy Build., vol. 129, pp. 452–470, 2016.

[27] I. Fatima, N. Javaid, S. Shafiq, S. Asif, M. H. Rahim, and S. Aslam, "Comparative study of meta-heuristic approaches towards utilization of home energy management," in Proc. Int. Conf. Comput., Math. Eng. Technol. (iCoMET), 2018, pp. 1–6.

[28] S. Aslam et al., "An efficient home energy management scheme using cuckoo search," in Proc. Int. Conf. P2P, Parallel, Grid, Cloud Internet Comput. (3PGCIC), Cham, Switzerland: Springer, 2017, pp. 167–178.

[29] I. Hussain et al., "Optimizing energy consumption in the home energy management system via a bio-inspired dragonfly algorithm and the genetic algorithm," Electronics, vol. 9, no. 3, p. 406, 2020, doi: 10.3390/electronics9030406.

[30] S. Balavignesh, C. Kumar, R. Sripriya, and T. Senjyu, "An enhanced coati optimization algorithm for optimizing energy management in smart grids for home appliances," Energy Rep., vol. 11, pp. 3695–3720, 2024.

[31] H. Youssef, S. Kamel, M. H. Hassan, L. Nasrat, and F. Jurado, "An improved bald eagle search optimization algorithm for optimal home energy management systems," Soft Comput., vol. 28, no. 2, pp. 1367–1390, 2024, doi: 10.1007/s00500-023-08328-0.

[32] S. Balavignesh, C. Kumar, S. Ueda, and T. Senjyu, "Optimization-based optimal energy management system for smart home in smart grid," Energy Rep., vol. 10, pp. 3733–3756, 2023, doi: 10.1016/j.egyr.2023.10.037.

[33] H. Youssef, S. Kamel, and M. H. Hassan, "Meta-heuristic-based home energy management system for optimizing smart appliance scheduling and electricity cost reduction in residential complexes," Neural Comput. Appl., vol. 36, no. 36, pp. 23077–23102, 2024.

[34] A. I. Ikram, A. Ullah, D. Datta, A. Islam, and T. Ahmed, "Optimizing energy

consumption in smart homes: Load scheduling approaches," IET Power Electron., vol. 17, no. 16, pp. 2656–2668, 2024.

[35] A. Ahmad et al., "An optimized home energy management system with integrated renewable energy and storage resources," Energies, vol. 10, no. 4, p. 549, 2017.

[36] A. O. Ali, M. R. Elmarghany, A. M. Hamed, M. N. Sabry, and M. M. Abdelsalam, "Optimized smart home energy management system: Reducing grid consumption and costs through real-time pricing and hybrid architecture," Case Stud. Therm. Eng., vol. 64, p. 105410, 2024.

[37] J. Brest, S. Greiner, B. Bošković, M. Mernik, and V. Žumer, "Self-adapting control parameters in differential evolution: A comparative study on numerical benchmark problems," IEEE Trans. Evol. Comput., vol. 10, no. 6, pp. 646–657, 2006.

[38] J. Zhang and A. C. Sanderson, "JADE: Adaptive differential evolution with optional external archive," IEEE Trans. Evol. Comput., vol. 13, no. 5, pp. 945–958, 2009.

[39] R. Tanabe and A. Fukunaga, "Success-history based parameter adaptation for differential evolution," in Proc. IEEE Congr. Evol. Comput. (CEC), 2013, pp. 71–78.

[40] W. Deng, X. Yang, L. Zou, M. Wang, Y. Liu, and Y. Li, "An improved self-adaptive differential evolution algorithm and its application," Chemometr. Intell. Lab. Syst., vol. 128, pp. 66–76, 2013.

[41] N. U. Rehman, N. Javaid, and Z. A. Khan, "An enhanced differential evolution based energy management system for smart grids," in Proc. 31st Int. Conf. Adv. Inf. Netw. Appl. Workshops (WAINA), 2017, pp. 132–137.

[42] P. Tiwari, V. N. Mishra, and R. P. Parouha, "Optimization of economic dispatch using updated differential evolution algorithm," Int. J. Inf. Technol., vol. 16, no. 4, pp. 2315–2329, 2024, doi: 10.1007/s41870-024-01730-3.